PERGAMON

International Journal of Solids and Structures 40 (2003) 6125–6142

INTERNATIONAL JOURNAL OF SOLIDS and STRUCTURES

www.elsevier.com/locate/ijsolstr

Magneto-thermo-elastic instability of ferromagnetic plates in thermal and magnetic fields

Xingzhe Wang [a], Jong S. Lee [b,*], Xiaojing Zheng [a]

[a] *Department of Mechanics, Lanzhou University, Lanzhou, Gansu, 730000, People's Republic of China*

[b] *Department of Civil and Environment Engineering, Hanyang University, Ansan, Kyunggi-Do 425-791, South Korea*

Received 27 September 2002; received in revised form 23 April 2003

Abstract

Based on a generalized variational principle for magneto-thermo-elasticity, a theoretical model is proposed to describe the coupled magneto-thermo-elastic interaction of soft ferromagnetic plates. Using the linearized theory of magneto-elasticity and perturbation technique, we analyze the magneto-elastic and magneto-thermo-elastic instability of simply supported ferromagnetic plates subjected to thermal and magnetic loadings. A coupled nonlinear finite element procedure is developed next to simulate the magneto-thermo-elastic behavior of a ferromagnetic plate. The effects of thermal and magnetic fields on the magneto-thermo-elastic bending and buckling is investigated in some detail.

Keywords: Soft ferromagnetic plates; Multi-fields interaction; Magneto-thermo-elastic bending and instability; Numerical analysis

1. Introduction

The classical thermo-elasticity of thin plates has been one of the most interesting fields of research (i.e. Sokolnikoff, 1939; Biot, 1956; Green and Lindsay, 1972). Recently, some investigators gave their attention to the magneto-thermo-elastic interaction in ferromagnetic plates as more ferromagnetic materials were used in technological applications, such as the first wall structure of thermo-nuclear reactors, electromagnetic energy storage devices and ferromagnetic shields, etc. (Lee et al., 1993). Paria (1967) and Parkus (1972) are the pioneers to study the field of magneto-thermo-elastic interaction. Misra et al. (1991) studied the stress in a solid cylinder of electroconductive medium with an axial magnetic field and a ramp-type thermal field. Banerjee and Roychoudhuri (1997) and Roychoudhuri and Banerjee (1998) investigated the magneto-thermo-elastic behavior of an infinite elastic and viscoelastic cylinder under a periodic loading. It should be noted that most of these studies are limited to a nonmagnetized medium.

* Corresponding author. Tel.: +82-31-400-5146; fax: +82-31-408-5140.
E-mail address: jonglee@hanyang.ac.kr (J.S. Lee).

0020-7683/$ - see front matter © 2003 Elsevier Ltd. All rights reserved.
doi:10.1016/S0020-7683(03)00297-X

When the magnetization of medium is considered, the analysis of multi-field coupling becomes more complex. Hutter and Pao (1974) developed the general theory of magneto-thermo-elastic bodies in applied magnetic fields and further reduced the basic equations through linearization. With the aid of the method of rational mechanics, Abd-alla and Maugin (1990) and Massalas (1991) respectively developed the equations of nonlinear magneto-thermo-elasticity for ferromagnetic media. However, in most of the aforementioned theories, the magnetic force arisen from the magnetization of a ferromagnetic medium is represented by the Maxwell magnetic stress tensor. Zhou and Zheng (1997) pointed out that there exists a configuration for which the usual Maxwell stress tensor may not be adequate for describing the magnetic force system of a ferromagnetic medium subjected to complex applied magnetic fields for which both the positive and negative magnetic stiffness manifest. They suggested a magneto-elastic model using the generalized variational principle to remedy the problem.

In this paper, we expand the generalized variational principle for magneto-elasticity to study the magneto-thermo-elastic interaction of soft ferromagnetic bodies under the action of applied thermal and magnetic fields. This expansion is achieved by using the magnetic energy and thermo-elastic free energy of the soft ferromagnetic material. In contrast to existing models (e.g. Abd-alla and Maugin, 1990; Massalas, 1991) which are based on Maxwell magnetic stress tensor, a new theoretical model for magneto-thermo-elastic interaction is proposed for soft ferromagnetic plates by taking geometrical nonlinearity and temperature-dependent magnetization into account. By means of the magnetic field perturbation technique and the finite element method, we analyze the interaction behavior of ferromagnetic plates in transverse and oblique magnetic fields. The magneto-thermo-elastic bending, buckling and post-buckling of the soft ferromagnetic plates are quantitatively investigated, and the effects of magnetic incident angle and temperature on the instability of the plates are examined in some detail.

2. The generalized energy functional

Consider an isotropic, homogeneous, linear magneto-elastic plate made of soft ferromagnetic material in both a stationary applied magnetic field $\mathbf{B}_0$ and a thermal field $T(x,y,z)$. The geometrical parameters of the plate are denoted respectively as the length a, the width b and the thickness h (see Fig. 1). Considering the dependence of the magnetic susceptibility or permeability on the thermal field (less than Curie temperature) and assuming that there is no electric field, charge distribution, or conduction current, we can write the magnetic constitutive relation for linear magnetic materials

$$\mathbf{M}^+ = \chi(T)\mathbf{H}^+, \quad \mathbf{B}^+ = \mu_0\mu_{\mathrm{r}}(T)\mathbf{H}^+ \quad \text{in } \Omega^+ \tag{1}$$

$$\mathbf{M}^- = \mathbf{0}, \quad \mathbf{B}^- = \mu_0\mathbf{H}^- \quad \text{in } \Omega^- \tag{2}$$

where Ω^+ and Ω^- represent the inside and outside regions of deformed plate respectively; $\mathbf{M}^+$ and $\mathbf{M}^-$ are respectively the magnetization vectors inside and outside the ferromagnetic medium; $\mathbf{B}^+, \mathbf{B}^-$ and $\mathbf{H}^+, \mathbf{H}^-$ are respectively the inside and outside magnetic induction vectors and magnetic field vectors; μ_0 and μ_{r} are the magnetic permeability of vacuum and the relative permeability of ferromagnetic medium respectively; χ is the susceptibility of the ferromagnetic medium and $\chi = \mu_{\mathrm{r}} - 1$.

Taking $\mathbf{u} = \{u, v, w\}$ as the displacement vector of the plate and S_0 as a closed surface far away from the region occupied by the ferromagnetic plate, we write the magnetic energy functional for the system as follows:

$$\Pi_{em}\{\phi, \mathbf{u}\} = \frac{1}{2}\int_{\Omega^+(\mathbf{u})} \mu_0\mu_{\mathrm{r}}(\nabla\phi^+)^2\,\mathrm{d}v + \frac{1}{2}\int_{\Omega^-(\mathbf{u})} \mu_0(\nabla\phi^-)^2\,\mathrm{d}v + \int_{S_0} \mathbf{n}\cdot\mathbf{B}_0\phi^-\,\mathrm{d}s \tag{3}$$

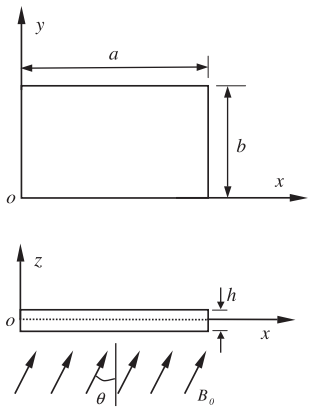

Fig. 1. The scheme of rectangular ferromagnetic plate.

in which ϕ is the magnetic scalar potential which satisfies $-\nabla\phi = \mathbf{H}$; and $\nabla = \partial/\partial x\mathbf{i} + \partial/\partial y\mathbf{j} + \partial/\partial z\mathbf{k}$ is the gradient operator.

With the assumptions that (i) all the elastic parameters are constants independent of the thermal field, (ii) there are no external forces acting on the ferromagnetic plate, and (iii) the von Karman theory of geometrically nonlinear thin plate may be used, the displacements of the thin plate can be expressed by the mid-plane deformation in the following forms:

$$u_1 = u - z\frac{\partial w}{\partial x}, \quad u_2 = v - z\frac{\partial w}{\partial y}, \quad u_3 = w \tag{4}$$

and the relations between the displacements and strains are given by

$$e_x = \frac{\partial u_1}{\partial x} + \frac{1}{2}\left(\frac{\partial u_3}{\partial x}\right)^2 = \varepsilon_x - z\chi_x \tag{5a}$$

$$e_y = \frac{\partial u_2}{\partial y} + \frac{1}{2}\left(\frac{\partial u_3}{\partial y}\right)^2 = \varepsilon_y - z\chi_y \tag{5b}$$

$$e_{xy} = \frac{1}{2}\left(\frac{\partial u_1}{\partial y} + \frac{\partial u_2}{\partial x} + \frac{\partial u_3}{\partial x}\frac{\partial u_3}{\partial y}\right) = \varepsilon_{xy} - z\chi_{xy} \tag{5c}$$

where

$$\varepsilon_x = \frac{\partial u}{\partial x} + \frac{1}{2}\left(\frac{\partial w}{\partial x}\right)^2, \quad \varepsilon_y = \frac{\partial v}{\partial y} + \frac{1}{2}\left(\frac{\partial w}{\partial y}\right)^2, \quad \varepsilon_{xy} = \frac{1}{2}\left(\frac{\partial u}{\partial y} + \frac{\partial v}{\partial x} + \frac{\partial w}{\partial x}\frac{\partial w}{\partial y}\right) \tag{6a}$$

$$\chi_x = \frac{\partial^2 w}{\partial x^2}, \quad \chi_y = \frac{\partial^2 w}{\partial y^2}, \quad \chi_{xy} = \frac{\partial^2 w}{\partial x \partial y} \tag{6b}$$

Thus, the functional of the thermo-elastic free energy functional of the system is given by

$$\Pi_{me}\{\phi, \mathbf{u}\} = \Pi^1_{me} + \Pi^2_{me} + \Pi^3_{me} \tag{7}$$

in which

$$\Pi^1_{me} = \frac{1}{2}\int_{S^+} C[(\varepsilon_x+\varepsilon_y)^2 + 2(1-v)(\varepsilon^2_{xy}-\varepsilon_x\varepsilon_y)]\,\mathrm{d}s \tag{8a}$$

$$\Pi^2_{me} = \frac{1}{2}\int_{S^+} D[(\chi_x+\chi_y)^2 + 2(1-v)(\chi^2_{xy}-\chi_x\chi_y)]\,\mathrm{d}s \tag{8b}$$

$$\Pi^3_{me} = -\frac{\alpha Y}{1-v}\int_{S^+}(\varepsilon_x+\varepsilon_y)\left[\int_{-h/2}^{h/2}(T-T_0)\,\mathrm{d}z\right]\mathrm{d}s + \frac{\alpha Y}{1-v}\int_{S^+}(\chi_x+\chi_y)\left[\int_{-h/2}^{h/2}(T-T_0)z\,\mathrm{d}z\right]\mathrm{d}s - \left[\frac{C_E}{2T_0}+\frac{\alpha^2 Y(1+v)}{(1-v)(1-2v)}\right]\int_{S^+}\int_{-h/2}^{h/2}(T-T_0)^2\,\mathrm{d}z\,\mathrm{d}s \tag{8c}$$

Here, Y and v are respectively the Young's modulus and the Poisson ratio; $C = Yh/(1-v^2)$ and $D = Yh^3/[12(1-v^2)]$ are the tensile and flexural rigidity of the thin plate, respectively; T_0 is the reference temperature; α is the coefficient of thermal expansion; C_E denotes the specific heat capacity; S^+ denotes the mid-plane of plate. By adding the magnetic energy functional and the thermo-elastic free energy, the total generalized magneto-thermo-elastic energy functional of the system is obtained as follows:

$$\Pi\{\phi,\mathbf{u}\} = \Pi_{em}\{\phi,\mathbf{u}\} + \Pi_{me}\{\phi,\mathbf{u}\} \tag{9}$$

With the stationary thermal field, the functional of potential energy of heat flux can be expressed as

$$\Pi_{th}\{T\} = \int_{\Omega^+}\left[\frac{1}{2}k(\nabla T)^2 - \rho h_T T\right]\mathrm{d}v - \int_{S_P}\left[(\lambda_1\bar{q} - \lambda_2 H_T\overline{T})T - \frac{1}{2}\lambda_2 H_T T^2\right]\mathrm{d}s \tag{10}$$

where k is the thermal conductivity of ferromagnetic material; ρ and h_T represent the material mass density and heat source density, respectively; H_T is the radiative coefficient; λ_1 and λ_2 are respectively the factors of heat flux and heat exchange on the boundary S_P; $\bar{q}$ and $\overline{T}$ are respectively the heat flux and environment temperature on S_P.

3. The governing equations

Let $\delta\phi$ be the admissible variation on magnetic potential function of the system. Then

$$\delta\phi = \delta\phi^+ = \delta\phi^- \quad \text{on } S \tag{11}$$

where S denotes the enclosed surface of the plate region Ω^+. From $\delta_\phi\Pi\{\phi,\mathbf{u}\} = 0$ and the arbitrariness of $\delta\phi$, one can obtain the governing equations and boundary conditions for the ferromagnetic body as follows:

$$\nabla^2\phi^+ = 0 \quad \text{in } \Omega^+(\mathbf{u}) \tag{12a}$$

$$\nabla^2\phi^- = 0 \quad \text{in } \Omega^-(\mathbf{u}) \tag{12b}$$

$$\phi^+ = \phi^-, \quad \mu_r\frac{\partial\phi^+}{\partial n} = \frac{\partial\phi^-}{\partial n} \quad \text{on } S \tag{12c}$$

$$-\nabla\phi^- = \frac{\mathbf{B}_0}{\mu_0} \quad \text{on } S_0 \tag{12d}$$

Analogously, we take $\delta\mathbf{u}$ as the admissible variation on the displacement of the plate and let $\delta_\mathbf{u}\Pi\{\phi,\mathbf{u}\} = 0$. With the arbitrariness of $\delta\mathbf{u}$ and the similar variational calculus procedure following Zhou

and Zheng (1997), we get the equilibrium equations and boundary conditions for a geometrically nonlinear ferromagnetic plate as follows:

$$\frac{\partial N_x}{\partial x}+\frac{\partial N_{xy}}{\partial y}=0,\quad \frac{\partial N_{xy}}{\partial x}+\frac{\partial N_y}{\partial y}=0 \tag{13a}$$

$$D\overline{\nabla}^2\overline{\nabla}^2 w+\frac{\alpha Y}{1-\nu}\int_{-h/2}^{h/2}\overline{\nabla}^2(T-T_0)z\,\mathrm{d}z-\left(N_x\frac{\partial^2 w}{\partial x^2}+2N_{xy}\frac{\partial^2 w}{\partial x\partial y}+N_y\frac{\partial^2 w}{\partial y^2}\right)=q_z^{em}(x,y,T) \tag{13b}$$

The corresponding boundary conditions are

(A) In-plane deformation:

(i) Movable boundary:

$$N_n=0\quad \text{on } \Gamma \tag{14a}$$

(ii) Immovable boundary:

$$u_n=0\quad \text{on } \Gamma \tag{14b}$$

(B) Bending deformation:

(i) Simply supported boundary:

$$w=0,\quad M_n=0\quad \text{on } \Gamma \tag{15a}$$

(ii) Fixed boundary:

$$w=0,\quad \frac{\partial w}{\partial n}=0\quad \text{on } \Gamma \tag{15b}$$

(iii) Free boundary:

$$M_n=0,\quad V_n=0\quad \text{on } \Gamma \tag{15c}$$

where M_n and V_n are respectively the bending moment and shearing force on the boundary Γ with the normal direction n; N_n and u_n denote the projections of the mid-plane internal force and displacement in the normal direction n on Γ, respectively; $\overline{\nabla}=\partial/\partial x\mathbf{i}+\partial/\partial y\mathbf{j}$ is the 2D gradient operator; N_x, N_y, N_{xy} and M_x, M_y, M_{xy} represent membrane and bending stress resultants of the thin plate respectively and are defined by

$$N_x=C(\varepsilon_x+v\varepsilon_y)-\frac{\alpha Y}{1-\nu}\int_{-h/2}^{h/2}(T-T_0)\,\mathrm{d}z \tag{16a}$$

$$N_y=C(\varepsilon_y+v\varepsilon_x)-\frac{\alpha Y}{1-\nu}\int_{-h/2}^{h/2}(T-T_0)\,\mathrm{d}z \tag{16b}$$

$$N_{xy}=C(1-v)\varepsilon_{xy} \tag{16c}$$

$$M_x=-D(\chi_x+v\chi_y)-\frac{\alpha Y}{1-\nu}\int_{-h/2}^{h/2}(T-T_0)z\,\mathrm{d}z \tag{17a}$$

$$M_y=-D(\chi_y+v\chi_x)-\frac{\alpha Y}{1-\nu}\int_{-h/2}^{h/2}(T-T_0)z\,\mathrm{d}z \tag{17b}$$

$$M_{xy}=-D(1-v)\chi_{xy} \tag{17c}$$

and the equivalent magnetic force exerted on the plate is given by

$$q_z^{em}(x,y,T) = \frac{\mu_0\chi(T)}{2}[\mu_r(T)(H_n^+)^2 - (H_\tau^+)^2]_{z=-h/2}^{z=h/2} \tag{18}$$

where H_n^+ and H_τ^+ represent respectively the normal and tangential components of $\mathbf{H}^+$ on the surface S of the ferromagnetic plate, which are related to the deformation of the plate and can be regarded as a transformation from the magnetic energy to the mechanical energy of the system.

Here, it should be pointed out that, in our derivation process of this section, the effects of thermal flux induced by magnetic field, temperature dependency of magnetic properties, and thermo-elastic coupling are neglected with stationary magnetic and thermal fields assumed. Consequently, we can get the governing equations directly from the potential energy functional of heat flux. Let δT be the admissible variation on the thermal functional of the system. Then, we have

$$\delta T = 0 \quad \text{on } S_T \tag{19}$$

Therefore, from $\delta\Pi_{th}\{T\} = 0$ and the arbitrariness of δT, the governing equation of heat conduction and boundary condition can be obtained as follows:

$$\nabla^2 T + \rho h_T = 0 \quad \text{in } \Omega^+ \tag{20a}$$

$$k\frac{\partial T}{\partial n} = \lambda_1\bar{q} + \lambda_2 H_T(T - \overline{T}) \quad \text{on } S_P \tag{20b}$$

4. Magneto-thermo-elastic buckling of ferromagnetic plates

The magneto-elastic buckling phenomenon of a soft ferromagnetic plate in transverse magnetic field ($\theta = 0°$) is known to us due to many investigations (e.g. Moon and Pao, 1968; Moon, 1984; Zhou et al., 1995; Lee, 1996; Zhou and Miya, 1998; Zheng et al., 1999). Here, we pay our attention to the magneto-thermo-elastic buckling of simply supported rectangular ferromagnetic plates under both the thermal and magnetic fields. The following analyses are based on the model developed in the previous section. For the sake of simplicity, the usual linear and infinitesimal strain theory for the ferromagnetic plate is adopted and the magnetic susceptibility χ is assumed independent of the thermal field. We also assume that the applied thermal and magnetic fields are stationary and uniform. The four edges of the plate are assumed to be fixed. By solving Eq. (13a), one can easily get the membrane stress resultants arisen from the thermal field as follows:

$$N_x = -\frac{\alpha YTh}{1-\nu}, \quad N_y = -\frac{\alpha YTh}{1-\nu}, \quad N_{xy} = 0 \tag{21}$$

Note that we take reference temperature $T_0 = 0$ for convenience.

A linearized theory (Pao and Yeh, 1973) is adopted for the distribution of the magnetic field inside and outside of the ferromagnetic plate. The magnetic field is divided into two parts: the rigid body state and the perturbed state. The former represents the magneto-statics solution for the undeformed plate and the latter is an added correction due to a small deformation of the plate, that is

$$\mathbf{H}^+ = \mathbf{H}_0^+ + \mathbf{h}^+ = -\nabla\Phi^+ - \nabla\phi^+ \quad \text{in } \Omega^+(\mathbf{u}) \tag{22a}$$

$$\mathbf{H}^- = \mathbf{H}_0^- + \mathbf{h}^- = -\nabla\Phi^- - \nabla\phi^- \quad \text{in } \Omega^-(\mathbf{u}) \tag{22b}$$

By considering the geometric characteristics of a thin plate (i.e. $h/a \ll 1$, $h/b \ll 1$) and neglecting the effect of the boundary magnetic field, we have

$$\nabla^2 \Phi^+ = 0 \quad \text{in } \Omega^+(\mathbf{u} = \mathbf{0}) \tag{23a}$$

$$\nabla^2 \Phi^- = 0 \quad \text{in } \Omega^-(\mathbf{u} = \mathbf{0}) \tag{23b}$$

$$\Phi^+ = \Phi^-, \quad \mu_r \frac{\partial \Phi^+}{\partial z} = \frac{\partial \Phi^-}{\partial z} \quad \text{on } z = \pm h/2 \tag{23c}$$

$$-\nabla \Phi^- = \frac{\mathbf{B}_0}{\mu_0} \quad \text{on } S_0 \text{ or at } \infty \tag{23d}$$

for the rigid body state and

$$\nabla^2 \phi^+ = 0 \quad \text{in } \Omega^+(\mathbf{u}) \tag{24a}$$

$$\nabla^2 \phi^- = 0 \quad \text{in } \Omega^-(\mathbf{u}) \tag{24b}$$

$$\mu_r \frac{\partial \phi^+}{\partial z} = \frac{\partial \phi^-}{\partial z} \quad \text{on } z = \pm h/2 \tag{24c}$$

$$\frac{\partial \phi^+}{\partial x} + H_{0z}^+ \frac{\partial w}{\partial x} = \frac{\partial \phi^-}{\partial x} + H_{0z}^- \frac{\partial w}{\partial x} \quad \text{on } z = \pm h/2 \tag{24d}$$

$$\frac{\partial \phi^+}{\partial y} + H_{0z}^+ \frac{\partial w}{\partial y} = \frac{\partial \phi^-}{\partial y} + H_{0z}^- \frac{\partial w}{\partial y} \quad \text{on } z = \pm h/2 \tag{24e}$$

$$\phi^- \to 0 \quad \text{on } S_0 \text{ or at } \infty \tag{24f}$$

for the perturbed state. As a consequence of Eqs. (23a)–(23d), we have

$$\mathbf{H}_0^+ = -\nabla \Phi^+ = \frac{\mathbf{B}_0}{\mu_0 \mu_r} \quad \text{in } \Omega^+(\mathbf{u} = \mathbf{0}) \tag{25a}$$

$$\mathbf{H}_0^- = -\nabla \Phi^- = \frac{\mathbf{B}_0}{\mu_0} \quad \text{in } \Omega^-(\mathbf{u} = \mathbf{0}) \tag{25b}$$

As for the plate deflection, a solution of the following form is chosen:

$$w = \sum_m \sum_n A_{mn} \sin \frac{m\pi x}{a} \sin \frac{n\pi y}{b} \tag{26}$$

where m and n denote positive integers, and A_{mn} is the coefficient of deflection amplitude. Upon substitution of Eqs. (25) and (26) into the corresponding boundary conditions of Eqs. (24d) and (24e), the distribution of the perturbed fields are given by

$$\begin{aligned} \mathbf{h}^+ &= -\nabla \phi^+ \\ &= \frac{B_0 \chi}{\mu_0 \mu_r} \sum_m \sum_n \frac{A_{mn}}{\Delta_{mn}} \frac{m\pi}{a} \cos \frac{m\pi x}{a} \sin \frac{n\pi y}{b} \cosh(k_{mn} z)\mathbf{i} + \frac{B_0 \chi}{\mu_0 \mu_r} \sum_m \sum_n \frac{A_{mn}}{\Delta_{mn}} \frac{n\pi}{b} \sin \frac{m\pi x}{a} \cos \frac{n\pi y}{b} \\ &\quad \times \cosh(k_{mn} z)\mathbf{j} + \frac{B_0 \chi}{\mu_0 \mu_r} \sum_m \sum_n \frac{k_{mn} A_{mn}}{\Delta_{mn}} \sin \frac{m\pi x}{a} \sin \frac{n\pi y}{b} \sinh(k_{mn} z)\mathbf{k} \end{aligned} \tag{27a}$$

$$\begin{aligned}\mathbf{h}^- &= -\nabla\phi^- \\ &= -\frac{B_0\chi}{\mu_0}\sum_m\sum_n \frac{A_{mn}}{\Delta_{mn}}\frac{m\pi}{a}\cos\frac{m\pi x}{a}\sin\frac{n\pi y}{b}\sinh\left(\frac{k_{mn}h}{2}\right)e^{k_{mn}(h/2-|z|)}\mathbf{i} - \frac{B_0\chi}{\mu_0}\sum_m\sum_n \frac{A_{mn}}{\Delta_{mn}}\frac{n\pi}{b} \\ &\quad\times \sin\frac{m\pi x}{a}\cos\frac{n\pi y}{b}\sinh\left(\frac{k_{mn}h}{2}\right)e^{k_{mn}(h/2-|z|)}\mathbf{j} - \frac{B_0\chi}{\mu_0}\mathrm{sgn}(z)\sum_m\sum_n \frac{k_{mn}A_{mn}}{\Delta_{mn}}\sin\frac{m\pi x}{a}\sin\frac{n\pi y}{b} \\ &\quad\times \sinh\left(\frac{k_{mn}h}{2}\right)e^{k_{mn}(h/2-|z|)}\mathbf{k} \end{aligned} \tag{27b}$$

where $\mathrm{sgn}(z)$ is the sign function, and

$$k_{mn} = \pi\sqrt{\left(\frac{m}{a}\right)^2 + \left(\frac{n}{b}\right)^2}, \quad \Delta_{mn} = \mu_r\sinh\frac{k_{mn}h}{2} + \cosh\frac{k_{mn}h}{2} \tag{28}$$

After taking the magnetic fields distributions of Eqs. (25a), (25b), (27a), and (27b) into the equivalent magnetic force of Eq. (18), we have

$$q_z^{em}(x,y) = \frac{2B_0^2\chi^2}{\mu_0\mu_r}\sum_m\sum_n \frac{k_{mn}A_{mn}}{\Delta_{mn}}\sinh\frac{k_{mn}h}{2}\sin\frac{m\pi x}{a}\sin\frac{n\pi y}{b} \tag{29}$$

The equilibrium equation of Eq. (13b), upon substituting Eqs. (21) and (29), is reduced to

$$\sum_m\sum_n A_{mn}\left[Dk_{mn}^4 - \frac{2B_0^2\chi^2k_{mn}}{\mu_0\mu_r\Delta_{mn}}\sinh\frac{k_{mn}h}{2} - \frac{\alpha YTh}{1-\nu}k_{mn}^2\right]\sin\frac{m\pi x}{a}\sin\frac{n\pi y}{b} = 0 \tag{30}$$

It should be noted from the above equation that $A_{mn} = 0$ or $w = 0$ when the applied magnetic field B_0 and thermal field T are small. This represents the unbending state as an equilibrium configuration for the ferromagnetic plate. As the field B_0 and/or T increase, however, there will be cases of $A_{mn} \neq 0$ or $w \neq 0$ which represents the buckling of the plate.

Case I: $T = 0$ and $B_0 \neq 0$. In this case, the ferromagnetic plate is placed in an applied magnetic field only. From Eq. (30), we find

$$Dk_{mn}^4 - \frac{2B_0^2\chi^2k_{mn}}{\mu_0\mu_r\Delta_{mn}}\sinh\frac{k_{mn}h}{2} = 0 \tag{31}$$

Thus, the critical magnetic field for magneto-elastic buckling ($m = n = 1$) is obtained as

$$B_{0\mathrm{cr}} = \left[\frac{\mu_0\mu_r\Delta_{11}\pi^3}{24(1-\nu^2)\chi^2\sinh(k_{11}/2)}\right]^{1/2}[1+(a/b)^2]^{3/4}(a/h)^{-3/2} \tag{32}$$

Noting that the magnetic permeability of most soft ferromagnetic materials is very large (e.g., $\chi > 10^4$ for iron) and the assumption of thin plate

$$\mu_r \approx \chi \gg 1, \quad \sinh(k_{11}h/2) \approx k_{11}h/2 \ll 1, \quad \cosh(k_{11}h/2) \approx 1 \tag{33}$$

Using the above relations, Eq. (32) is further reduced in nondimensional form

$$B_{\mathrm{cr}}^* = \frac{B_{0\mathrm{cr}}}{\sqrt{\mu_0 Y}} = \frac{\pi}{2}\left[\frac{\pi}{6(1-\nu^2)}\right]^{1/2}[1+(a/b)^2]^{3/4}(a/h)^{-3/2} \tag{34}$$

which shows that the critical magnetic field B_{cr}^* varies with $-3/2$ power of the geometric parameter a/h. It agrees with the Moon and Pao (1968) and Dalamangas (1983).

Case II: $T \neq 0$ and $B_0 = 0$. In this case, the ferromagnetic plate is placed in an applied thermal field only. From Eq. (30), we find

$$Dk_{mn}^4 - \frac{\alpha YT}{1-v}k_{mn}^2 = 0 \tag{35}$$

and the critical value of thermal field (dimensionless) for the thermo-elastic buckling is obtained by

$$T_{\mathrm{cr}}^* = \alpha T_{\mathrm{cr}} = \frac{\pi^2}{12(1+v)}[1+(a/b)^2](a/h)^{-2} \tag{36}$$

Case III: $T \neq 0$ and $B_0 \neq 0$. The ferromagnetic plate is placed in both the applied thermal field and magnetic field. In this case, we obtain the effect of the thermal field on the critical magnetic field for magneto-elastic buckling, and the effect of the magnetic field on the critical thermal field for thermo-elastic buckling as follows:

$$B_{\mathrm{cr}}^* = \frac{\pi^3 h^3}{24(1-v^2)a^3} - \left[\frac{\pi h T^*}{2(1-v)a}\right]^{1/2}[1+(a/b)^2]^{1/4} \tag{37a}$$

$$T_{\mathrm{cr}}^* = \frac{\pi^2}{12(1+v)}[1+(a/b)^2](a/h)^{-2} - \frac{2(1-v)(B^*)^2}{\pi\sqrt{1+(a/b)^2}}\frac{a}{h} \tag{37b}$$

and the characteristic curve of magneto-thermo-elastic buckling for the ferromagnetic plate as follows:

$$\left(\frac{B^*}{B_{\mathrm{cr}}^*}\right)^2 + \frac{T^*}{T_{\mathrm{cr}}^*} = 1 \tag{38}$$

where B^* and T^* are the dimensionless variables of magnetic and thermal field, respectively. The corresponding deflected configuration of the magneto-thermo-elastic buckling is expressed as

$$w = A_{11}\sin\frac{\pi x}{a}\sin\frac{\pi y}{b} \tag{39}$$

The logarithmic curves for critical values of magneto-elastic and thermo-elastic buckling of the simply supported plate are plotted as a function of the geometrical parameter a/h in Fig. 2(a) and (b) respectively.

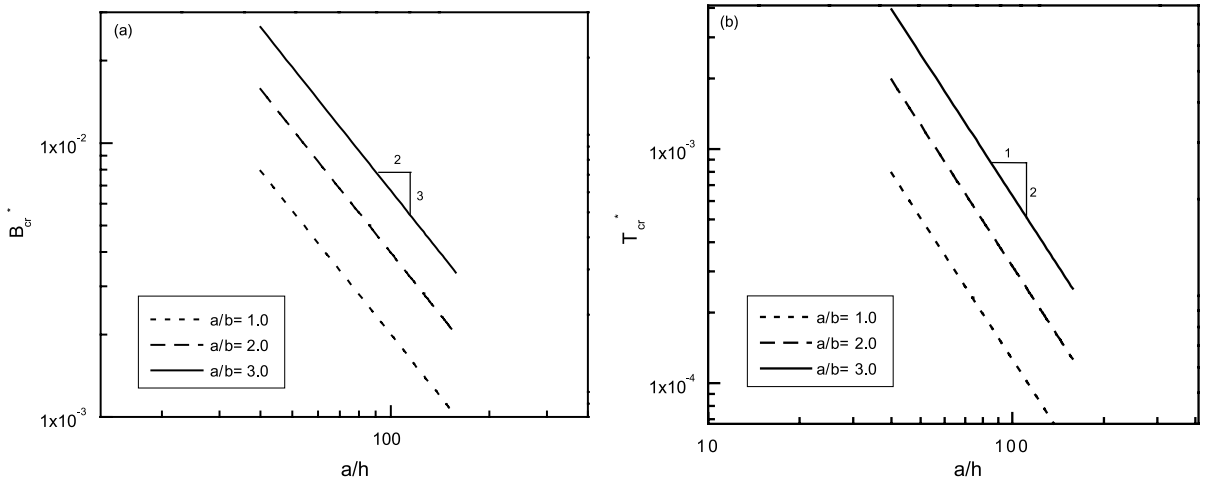

Fig. 2. The logarithmic curve for critical value vs. the geometric parameter a/h: (a) magneto-elastic buckling; (b) thermo-elastic buckling.

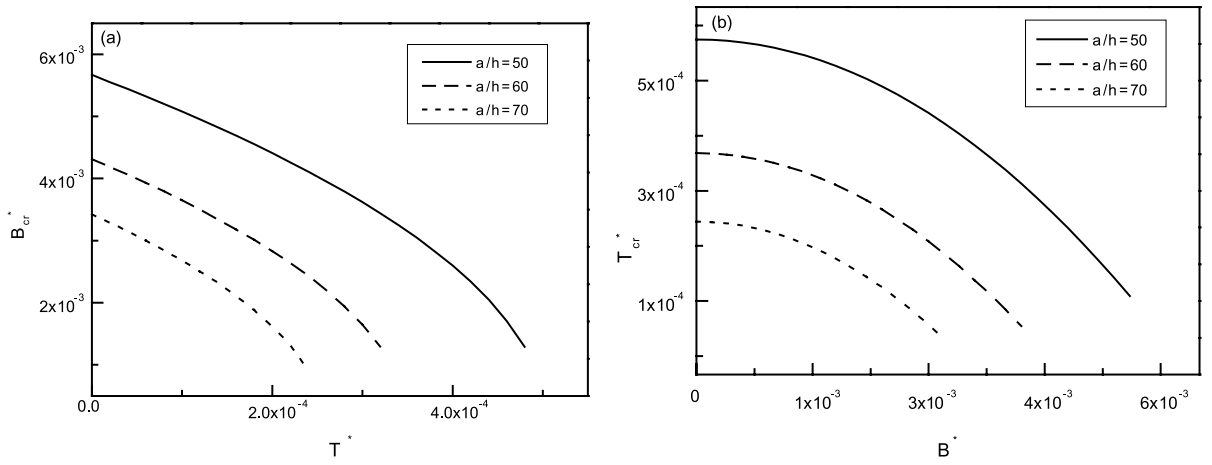

Fig. 3. The buckling of magneto-elasticity and thermo-elasticity depending on thermal and magnetic field ($a/b = 1.0$): (a) the effect of T^* on B^*_{cr}; (b) the effect of B^* on T^*_{cr}.

These show that the critical values for magneto-elastic buckling decrease with $-3/2$ power of the ratios a/h, while those for thermo-elastic buckling decrease with -2 power of the ratios a/h. Fig. 3(a) shows the effect of the thermal field on the magneto-elastic buckling while Fig. 3(b) shows the effect of magnetic field on the thermo-elastic buckling. Fig. 4 presents further the characteristic curve of magneto-thermo-elastic buckling where B^*_{cr} and T^*_{cr} denote the critical magnetic and thermal field respectively for the plate subjected to a magnetic or thermal field only. In the figure, the region enclosed by the characteristic curve and the ordinate implies the stable region where the magneto-thermo-elastic buckling would not take place.

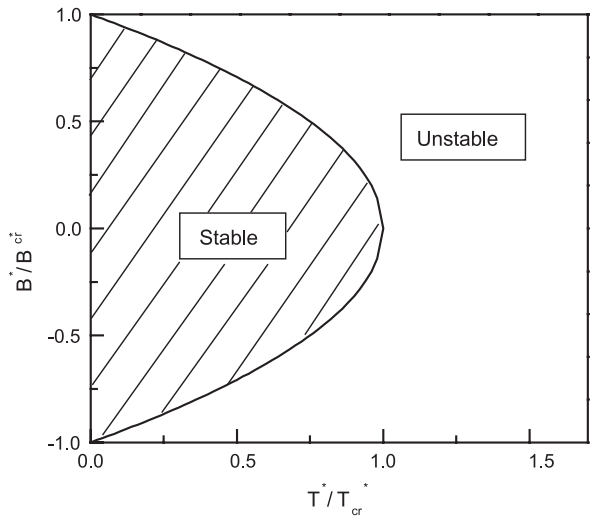

Fig. 4. The characteristic curve of magneto-thermo-elastic buckling.

5. The finite element analysis

In general, it is not easy to obtain analytical solutions to a magneto-thermo-elastic problem with combined fields since the field equations are strongly coupled and nonlinear due to the interactions among the fields. The exact solution or quantitative analysis is limited to structures of simple geometry and simple support conditions where the edge effect of magnetic field can be neglected. However, there are many ferromagnetic structures of finite size with complex field configuration in engineering applications, thereby necessitating a numerical means. In this section, we develop a numerical program based on the finite element method to analyze the elastic, magnetic, and thermal field distributions of the plate. An iterative method is employed to take care of the nonlinearities arisen from the field-structure interaction.

5.1. FEM formulation for magnetic field

Firstly, we will analyze the magnetic field distributions in regions Ω^+ and Ω^- that are influenced by the magnetization and deformation of the ferromagnetic plate. For a given deflected state of the ferromagnetic plate, the magnetic field distribution (solution of Eqs. (12a)–(12d)) minimizes the magnetic-energy functional $\Pi_{em}\{\phi, \mathbf{u}\}$ for the ferromagnetic system. We discretize the 3D regions of Ω^+ and Ω^- into finite elements setting the mid-plane and the surface of the plate located on the surface of the elements. Here, we adopt 20-node hexahedron elements and the corresponding shape function $[\mathbf{N}^{em}(x,y,z)]_e$. For each element, we have

$$\phi(x,y,z) = [\mathbf{N}^{em}(x,y,z)]_e[\mathbf{\Phi}]_e \tag{40}$$

where $[\mathbf{\Phi}]_e$ is a column matrix which consists of the value of $\phi(x,y,z)$ on each node of the element e. Upon substituting Eq. (40) into the discretized form of magnetic energy for the system, we have

$$\Pi_{em}\{\phi, \mathbf{u}\} = \sum_e \frac{1}{2}[\mathbf{\Phi}]_e^{\mathrm{T}}[\mathbf{K}^{em}]_e[\mathbf{\Phi}]_e - \sum_e [\mathbf{\Phi}]_e^{\mathrm{T}}[\mathbf{P}]_e \tag{41}$$

where $[\mathbf{K}^{em}]_e$ and $[\mathbf{P}]_e$ are respectively the magnetic stiffness matrix and the inhomogeneous term for element e, and are expressed as

$$[\mathbf{K}^{em}]_e = \begin{cases} \int_{\Omega_e} \mu_0\mu_{\mathrm{r}}[\nabla\mathbf{N}^{em}]_e^{\mathrm{T}}[\nabla\mathbf{N}^{em}]_e \,\mathrm{d}v & \Omega_e \in \Omega^+(\mathbf{u}) \\ \int_{\Omega_e} \mu_0[\nabla\mathbf{N}^{em}]_e^{\mathrm{T}}[\nabla\mathbf{N}^{em}]_e \,\mathrm{d}v & \Omega_e \in \Omega^-(\mathbf{u}) \end{cases} \tag{42a}$$

$$[\mathbf{P}]_e = \begin{cases} \int_{S_e} \mu_0\mathbf{n}\cdot\mathbf{B}_0[\mathbf{N}^{em}]_e^{\mathrm{T}} \,\mathrm{d}s & S_e \in S_0 \\ \mathbf{0} & S_e \notin S_0 \end{cases} \tag{42b}$$

From $\delta_\phi\Pi_{em}\{\mathbf{u}, \phi\} = 0$, one can get the algebraic equation for magnetic scalar potential in the form

$$[\mathbf{K}^{em}][\mathbf{\Phi}] = [\mathbf{P}] \tag{43}$$

Here, $[\mathbf{K}^{em}]$ is the global magnetic stiffness matrix; $[\mathbf{\Phi}]$ is a column matrix of the unknown nodal values of the magnetic potential; $[\mathbf{P}]$ is the column matrix or "force" vector related to the applied magnetic field on S_0. Since the region $\Omega^+(\mathbf{u})$ represents the deformed plate and the magnetic permeability is a function of the thermal field, it is obvious that

$$[\mathbf{K}^{em}] = [\mathbf{K}^{em}(\mathbf{u}, T)] \tag{44}$$

5.2. FEM formulation for thermal field

Here, we develop a finite element formulation to compute the thermal field. The heat conduction equation together with the corresponding boundary conditions, Eqs. (20a) and (20b), constitute a boundary-value problem that minimizes the potential functional of heat flux of the system. The magnetic field elements in region Ω^+ can be taken as the thermal field elements with the temperature function instead of the magnetic scalar potential as the unknown values at the nodes of each element. The temperature for each element is given by

$$T(x,y,z) = [\mathbf{N}^{th}(x,y,z)]_e[\mathbf{T}]_e \tag{45}$$

in which $[\mathbf{N}^{th}(x,y,z)]_e$ is the shape function of the thermal field element e; and $[\mathbf{T}]_e$ is the column matrix which consists of the value of $T(x,y,z)$ at each node.

Substituting Eq. (45) into the discretized form of the thermal flux potential for the system leads to

$$\Pi_{th}\{T\} = \frac{1}{2}\sum_e [\mathbf{T}]_e^{\mathrm{T}}[\mathbf{K}_h^{th}]_e[\mathbf{T}]_e - \sum_e [\mathbf{T}]_e^{\mathrm{T}}[\mathbf{Q}_h]_e - \frac{1}{2}\sum_{e_0}[\mathbf{T}]_e^{\mathrm{T}}[\mathbf{K}_s^{th}]_e[\mathbf{T}]_e + \sum_{e_0}[\mathbf{T}]_e^{\mathrm{T}}[\mathbf{Q}_s]_e \tag{46}$$

where e and e_0 represent the thermal field elements inside and on the boundary of the plate, respectively; $[\mathbf{K}_h^{th}]_e$ is the heat conduction stiffness matrix; $[\mathbf{K}_s^{th}]_e$ is the thermal stiffness matrix due to the heat exchange on the boundary S_P; and $[\mathbf{Q}_h]_e$ and $[\mathbf{Q}_s]_e$ are respectively the inhomogeneous terms from the heat source loading inside the plate and the heat flux and the heat exchange on the boundary. These matrices can be written as follows:

$$[\mathbf{K}_h^{th}]_e = \int_{\Omega_e^+} k[\nabla \mathbf{N}^{th}]^{\mathrm{T}}[\nabla \mathbf{N}^{th}]\,\mathrm{d}v \tag{47a}$$

$$[\mathbf{K}_s^{th}]_e = \int_{S_e 0} \lambda_2 H_T[\mathbf{N}^{th}]^{\mathrm{T}}[\mathbf{N}^{th}]\,\mathrm{d}s \tag{47b}$$

$$[\mathbf{Q}_h]_e = \int_{\Omega_e^+} \rho h_T[\mathbf{T}^{th}]^{\mathrm{T}}\,\mathrm{d}v \tag{47c}$$

$$[\mathbf{Q}_s]_e = \int_{S_e} (\lambda_1 \bar{q} - \lambda_2 H_T \overline{T})[\mathbf{N}^{th}]^{\mathrm{T}}\,\mathrm{d}s \tag{47d}$$

From $\delta\Pi_{th}\{T\} = 0$, a matrix equation for the thermal field may be obtained as

$$[\mathbf{K}^{th}(\mathbf{u})][\mathbf{T}] = [\mathbf{Q}(\mathbf{u})] \tag{48}$$

where $[\mathbf{K}^{th}(\mathbf{u})]$ is the global heat conduction stiffness matrix; $[\mathbf{T}]$ is the column matrix which consists of the temperature values at the nodes; and $[\mathbf{Q}(\mathbf{u})]$ is the column matrix related to the heat source, heat flux and heat exchange.

5.3. FEM formulation for plate

Taking the rectangular areas of the 3D hexahedron elements in the mid-plane of plates as the plate elements, we can reduce the differential equations (13a) and (13b) with the corresponding boundary conditions into a matrix equation

$$[\mathbf{K}^{me}][\mathbf{U}] = [\mathbf{R}] \tag{49}$$

where $[\mathbf{K}^{me}]$ is the stiffness matrix for deformation of the plate; $[\mathbf{U}]$ is a column matrix of unknown nodal values of the plate deformation; and $[\mathbf{R}]$ is a column matrix of the load which is related to the magnetic force. It should be noted that $[\mathbf{K}^{me}]$ is a function of the deformation whereas $[\mathbf{R}]$ is a function of the magnetic and deformation fields, that is

$$[\mathbf{K}^{me}] = [\mathbf{K}^{me}([\mathbf{U}])], \quad [\mathbf{R}] = [\mathbf{R}([\mathbf{\Phi}([\mathbf{U}])])] \tag{50}$$

5.4. Iterative method

As shown in Eqs. (43), (44), and (48)–(50), the magneto-thermo-elastic problem for ferromagnetic plates shows strong nonlinearity due to multi-field couplings. Here, the Newton–Raphson method is employed to solve Eqs. (43) and (49). The iterative equation can be written as

$$[\mathbf{U}_{m+1}] = [\mathbf{U}_m] - [\overline{K}_m^{me}]^{-1}[\mathbf{\Psi}([\mathbf{U}_m])] \tag{51}$$

where the subscripts m and $m+1$ denote the numbers of iteration, $[\mathbf{\Psi}([\mathbf{U}_m])]$ is denoted by

$$[\mathbf{\Psi}([\mathbf{U}_m])] = [\mathbf{K}^{me}([\mathbf{U}_m])][\mathbf{U}_m] - [\mathbf{R}([\mathbf{K}^{em}([\mathbf{U}_m])]^{-1}[\mathbf{P}], T)] \tag{52}$$

and $[\overline{\mathbf{K}}_m^{me}]$ is the tangent stiffness matrix is given by

$$[\overline{\mathbf{K}}_m^{me}] = \left[\frac{\partial \mathbf{\Psi}([\mathbf{U}_m])}{\partial [\mathbf{U}]}\right] \tag{53}$$

In view of the theory, once the tangent stiffness matrix, Eq. (53), is obtained, one can get the magneto-elastic deformation of the ferromagnetic plate from Eq. (51). However, the tangent stiffness matrix $[\overline{\mathbf{K}}_m^{me}]$ is not known a priori because the coupling between the magnetic force exerted on the plate and the deformation of the plate is implicit. An iterative technique is adopted again to solve this nonlinear interaction problem. Eq. (52) can be rewritten as

$$[\mathbf{\Psi}([\mathbf{U}_m^{n+1,n}])] = [\mathbf{K}^{me}([\mathbf{U}_m^{n+1}])][\mathbf{U}_m^{n+1}] - [\mathbf{R}([\mathbf{K}^{em}([\mathbf{U}_m^{n}])]^{-1}[\mathbf{P}], T)] \tag{54}$$

where the superscripts n and $n+1$ denote the numbers of iteration. Thus, we can rewrite Eq. (53) in the form

$$[\overline{\mathbf{K}}_m^{me}]_{n+1,n} = \left[\frac{\partial \mathbf{\Psi}([\mathbf{U}_m^{n+1,n}])}{\partial [\mathbf{U}^{n+1}]}\right] \tag{55}$$

Substituting of Eqs. (54) and (55) into Eq. (51) leads to

$$[\mathbf{U}_{m+1}^{n+1}] = [\mathbf{U}_m^{n+1}] - [\overline{\mathbf{K}}_m^{me}]_{n+1,n}^{-1}[\mathbf{\Psi}([\mathbf{U}_m^{n+1,n}])] \tag{56}$$

We repeat the calculation given by the above equation until the following conditions are satisfied:

$$\|\mathbf{\Psi}([\mathbf{U}_m^{n+1,n}])\| < \varepsilon_1, \quad \|[\mathbf{U}_{m+1}^{n+1}] - [\mathbf{U}_m^{n+1}]\| < \varepsilon_2 \tag{57}$$

where $0 < \varepsilon_1 \ll 1$ and $0 < \varepsilon_2 \ll 1$ are the prescribed limits. Finally we obtain the magneto-thermo-elastic deformation of the ferromagnetic plate under magnetic field $\mathbf{B}_0$ and thermal field T by

$$[\mathbf{U}] = \lim_{m,n\to\infty} [\mathbf{U}_m^n] \tag{58}$$

6. Numerical results and discussions

Some numerical examples are presented here to show the magneto-thermo-elastic behavior (viz., bending, buckling and post-buckling) of a rectangular ferromagnetic plate subjected to magnetic and thermal fields (shown in Fig. 1). The geometric and material parameters are listed in Table 1.

We first consider a numerical example of a ferromagnetic plate with a prescribed thermal field. The thermal boundary conditions are given by

$$T = P\cos(\pi y/b), \quad \text{at } x = 0; \qquad T = 0, \quad \text{at } x = a \tag{59a}$$

$$\partial T/\partial y = 0, \quad \text{at } y = 0, b \tag{59b}$$

In this case, the thermal field distribution of the ferromagnetic plate is independent of the thickness of the plate, that is, $T = T(x, y)$. Fig. 5 shows the maximum deflection of the plate vs. applied magnetic field B_0^* (dimensionless $B_0^* = B_0/\sqrt{\mu_0 Y} \times 10^4$) for the selected temperature intensities. From the figure, one can find that the magneto-thermo-elastic buckling takes place and its behavior is similar to the magneto-elastic buckling where only the magnetic field is applied. When the applied magnetic-field intensity increases beyond the critical value, the deflection of the plate increases along the post-buckling configuration and the plate still has some load bearing capacity. Fig. 6 shows the critical magnetic fields as a function of the thermal intensity P. One can see that the higher the thermal intensity the smaller the critical magnetic field, as the increasing thermal intensity enhances the membrane stress in the plate. As shown in the figure, the buckling value at $P = 200$ °C is almost half of that at $P = 0$ °C (without any thermal effect). Fig. 7 shows

Table 1
Geometric and material parameters of ferromagnetic plate

Length, a (m)	Width, b (m)	Thickness, h (m)	Young's modulus, Y (MPa)	Poisson's ratio, v	Relative permeability, μ_r	Thermal coefficient, α (1/°C)
0.1	0.1	0.001	1.2×10^5	0.3	1000	1.0×10^{-5}

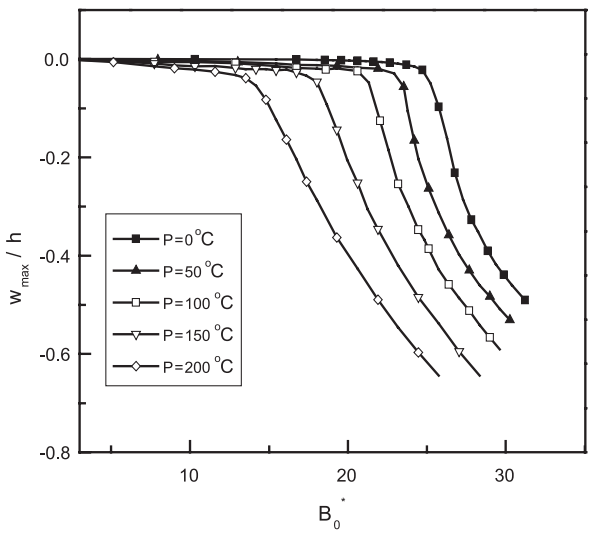

Fig. 5. The curve of the maximum deflection vs. applied magnetic intensity (transverse magnetic field).

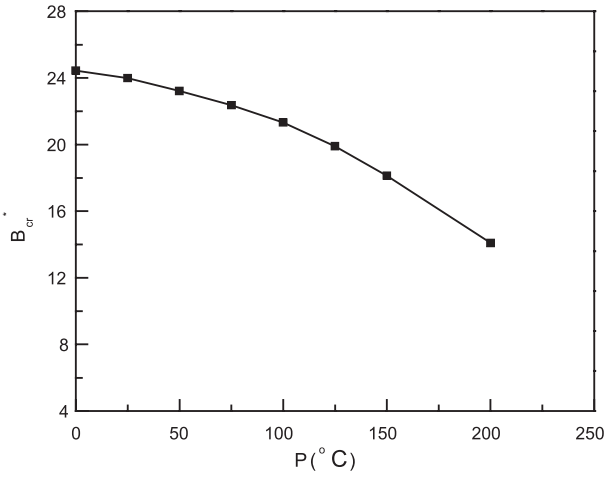

Fig. 6. The critical magnetic field of magneto-thermo-elastic buckling vs. thermal field (transverse magnetic field).

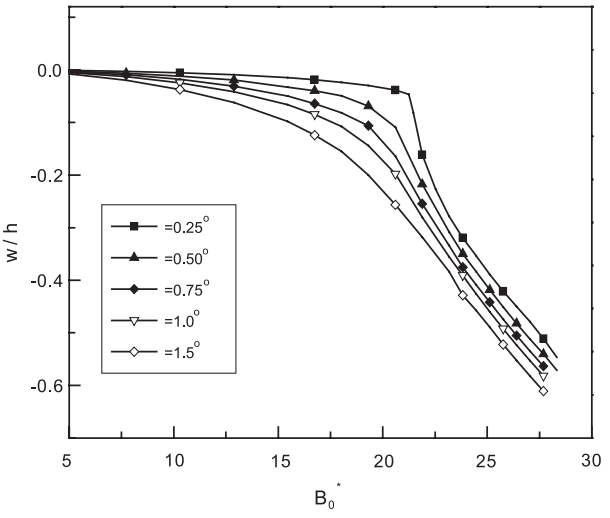

Fig. 7. The deflection curve of magneto-thermo-elastic bending ($P = 100$ °C).

the deflection of the plate at a point ($x = a/4$, $y = b/2$) as a function of the magnetic-field intensity for several incident angles. One can see that the incident angle can significantly influence the magneto-thermo-elastic behavior of the plate. As shown in the figure, the buckling takes place for a small incident angle whereas the plate shows mostly bending for relatively large angles.

The second numerical example involves a prescribed thermal condition, in which the upper and lower surfaces of the plate have different temperatures. The corresponding boundary conditions are given as follows:

$$T = T_0 + \delta T, \quad \text{at } z = h/2; \qquad T = T_0, \quad \text{at } z = -h/2 \tag{60a}$$

$$k\partial T/\partial y = H_T(T - T_0), \quad \text{at } x = 0, a \text{ and } y = 0, b \tag{60b}$$

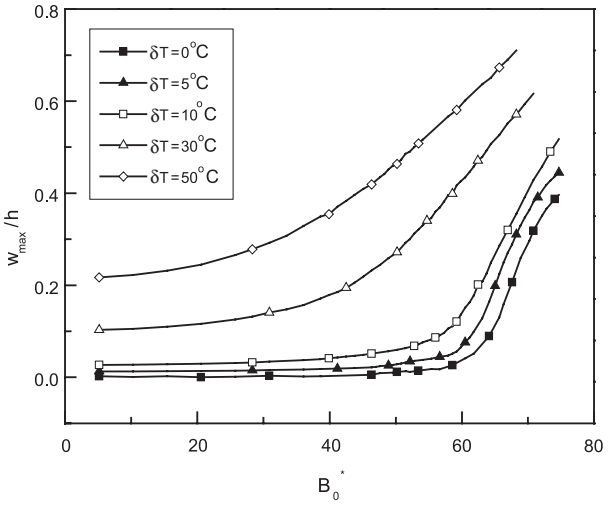

Fig. 8. The curve of the maximum deflection vs. applied magnetic-field intensity (transverse magnetic field).

where $T_0 = 20$ °C is chosen for the reference temperature; the heat conduction coefficient $k = 10.0$ W/m °C; the radiative coefficient $H_T = 0.1$ W/m^2 °C; and the thickness of plate $h = 0.002$ m. Other geometric and material parameters of the plate are the same as listed in Table 1. In addition, to study the effect of the thermal field on the magnetization through the magneto-thermo-elastic interaction, two different magnetic constitutive relations are used: (a) $B = \mu_0\mu_r H$ with $\mu_r = 1000$, and (b) $B = \mu_0\mu_r(T)H$ with $\mu_r(T) = \beta_1 + \beta_2 T$. The case (a) is the usual linear, isotropic magnetization relation for ferromagnetic media and the case (b) takes into account the effect of temperature on magnetization in which $\beta_1 = 600$ and $\beta_2 = 20$ (1/°C).

For a transverse magnetic field, the maximum deflection of the simply supported plate is plotted as a function of the magnetic-field intensity in Fig. 8 for selected values of δT for case (a). One can find that the plate buckles for zero or small temperature-difference of the plate (i.e., $\delta T = 0, 5, 10$ °C), whereas the plate exhibits bending only for large values of δT (i.e., $\delta T = 30$, 50 °C). We next investigate the effects of the magnetic-field incident angle and the magnetization relations on the mechanical behavior of the plate.

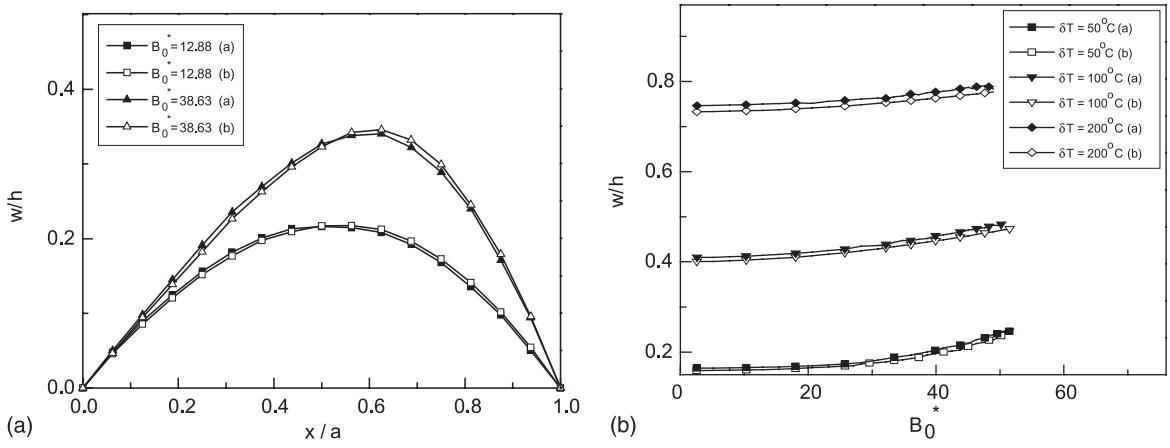

Fig. 9. The bending of the plate in an oblique magnetic field with a small incident angle ($\theta = 3.0°$): (a) the deflection curve ($\delta T = 50$ °C, $y = b/2$); (b) the deflection vs. magnetic field.

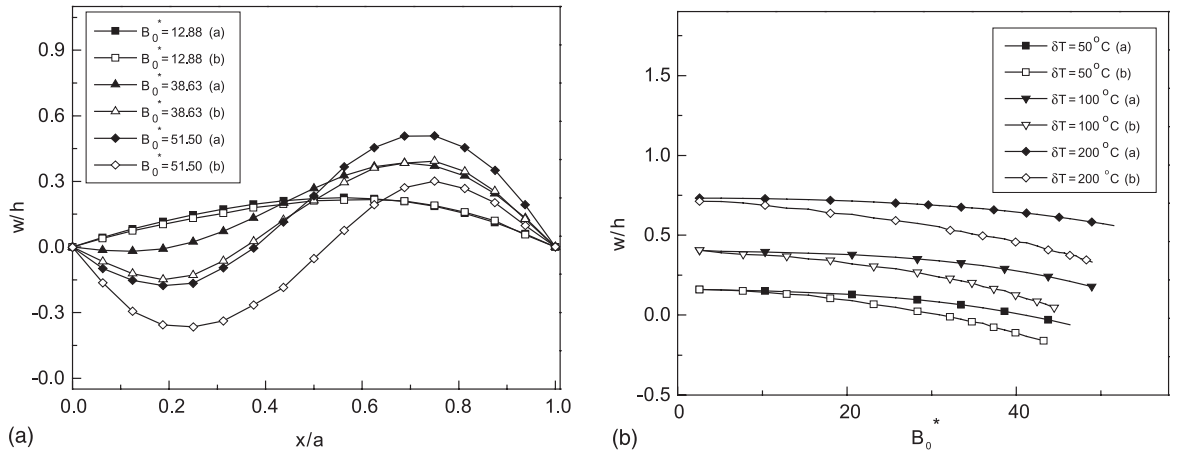

Fig. 10. The bending of the plate in an oblique magnetic field with a large incident angle ($\theta = 10.0°$): (a) the deflection curve ($\delta T = 50$ °C, $y = b/2$); (b) the deflection vs. magnetic field.

Fig. 9(a) and (b) show the deflection curves in the middle of the plate ($y = b/2$) and the deflection at a point ($x = a/4$, $y = b/2$) respectively for a small oblique angle (i.e., $\theta = 3.0°$). One can find that, from these figures, there is not significant difference between the two cases of magnetization relations adopted. In this case, the plate exhibits mostly thermo-elastic bending with the characteristic deflection of half-wave type due to the temperature difference between the upper and lower surfaces of the plate. This also can be found from Fig. 9(b) which exhibits similar behavior between the two constitutive relatives and that the bending of the plate increases with the applied magnetic field B_0^* slowly, especially for the larger temperature difference ($\delta T = 200$ °C). Now we carry out a similar analysis using a large incident angle ($\theta = 10.0°$). Fig. 10(a) and (b) show the deflection curves at $y = b/2$ and the deflection at a point ($x = a/4$, $y = b/2$) respectively. The figures display a marked effect of the magnetization relations as well as the intensity of the applied field on the bending of the plate. As shown in Fig. 10(a), the deflection curve is a half-wave type (typical of thermo-elastic bending) for small applied magnetic fields but it becomes whole wave type (typical of magneto-elastic bending in a oblique field, see Zheng et al., 1999) when the strong magnetic field is applied. As shown in Fig. 10(b), the bending of the plate with magnetization relations (a) and (b) show notable differences which become larger as the applied magnetic-field intensity increases.

7. Conclusions

For a soft ferromagnetic plate with geometrical nonlinearity and temperature-dependent magnetization, a theoretical model for magneto-thermo-elastic boundary-value problem is developed based on a generalized variational principle. The fundamental equations thus developed are nonlinear and coupled. By adopting an appropriate linearization and magnetic field perturbation method, the magneto-thermo-elastic buckling of a soft ferromagnetic rectangular plate with simple supports is analyzed. The magneto-thermo-elastic stability regions and the critical field intensities which are dependent on the geometrical parameters and applied magnetic or thermal field are obtained. A coupled nonlinear finite element program is developed to simulate the magneto-thermo-elastic behavior of ferromagnetic plates. The results show that the plate subjected simultaneously to a transverse magnetic field and a thermal field buckles when the applied magnetic field reaches a critical value and that the thermal field decreases the critical field. In the case where the plate is subjected to an oblique magnetic fields, it buckles for a small incident angle while it exhibits

mostly magneto-thermo-elastic bending for a larger incident angle. For larger incident angles and stronger applied magnetic fields, the temperature-dependent magnetization effects markedly on the bending and should be noted in the analysis of the plate in the multi-field interaction environment.

Acknowledgements

This research was supported in part by the National Outstanding Youth Fund (No. 19725207) of China and in part by the Brain Korea 21 and the National Research Laboratory Programs of Korea. The authors gratefully acknowledge the supports.

References

Abd-alla, A.N., Maugin, G.A., 1990. Nonlinear equations for thermoelastic magnetizable conductors. Int. J. Engng. SCI 28 (7), 589–603.

Banerjee, S., Roychoudhuri, S.K., 1997. Magneto-thermo-elastic interactions in an infinite isotropic elastic cylinder subjected to a periodic loading. Int. J. Engng. Sci. 35 (4), 437–444.

Biot, M.A., 1956. Thermoelasticity and irreversible thermodynamics. J. Appl. Phys. 27, 240–247.

Dalamangas, A., 1983. Magnetoelastic stability and vibration of ferromagnetic thin plates in a transverse magnetic field. Mech. Res. Commun. 10 (5), 279–286.

Green, A.E., Lindsay, K.A., 1972. Thermoelasticity. J. Elasticity 2, 1–7.

Hutter, K., Pao, Y.H., 1974. A dynamical theory for magnetizable elastic solids with thermal and electrical conduction. J. Elasticity 4 (2), 89–114.

Lee, J.S., 1996. Dynamic stability of conduction beam-plates in transverse fields. J. Engng. Mech. 122 (2), 89–94.

Lee, J.S., Maugin, G.A., Shindo, Y., 1993. Mechanics of Electromagnetic Materials and Structures. ASME, New York.

Massalas, C.V., 1991. A note on magneto-thermo-elastic interactions. Int. J. Engng. Sci. 29 (10), 1217–1229.

Misra, J.C., Samanta, S.C., Chakrabarti, A.K., 1991. Magnetic–mechanical interaction in an aeolotropic solid cylinder subjected to a ramp-type heating. Int. J. Engng. Sci. 29 (9), 1065–1075.

Moon, F.C., 1984. Magneto-solid Mechanics. John Wiley and Sons, New York.

Moon, F.C., Pao, Y.H., 1968. Magnetoelastic buckling of a thin plate. ASME J. Appl. Mech. 35 (1), 53–58.

Pao, Y.H., Yeh, C.S., 1973. A linear theory for soft ferromagnetic elastic solids. Int. J. Engng. Sci. 11 (4), 415–436.

Paria, G., 1967. Magneto-elasticity and magneto-thermo-elasticity. In: Advances in Applied Mechanics, vol. 10. Academic Press, New York, pp. 73–112.

Parkus, H., 1972. Magnetothermoelasticity, Lecture Note, CISM, Udine. Spring, Vienna.

Roychoudhuri, S.K., Banerjee, S., 1998. Magneto-thermo-elastic interaction in an infinite viscoelastic cylinder of temperature-rate dependent material subjected to a periodic loading. Int. J. Engng. Sci. 35 (5–6), 635–643.

Sokolnikoff, E.S., 1939. Thermal stresses in elastic plates. Trans. Am. Math. Soc. 45, 235–255.

Zheng, X.J., Zhou, Y.H., Wang, X., Lee, J.S., 1999. Bending and buckling of ferroelastic plates. J. Engng. Mech. 125, 180–185.

Zhou, Y.H., Miya, K., 1998. A theoretical prediction of natural frequency of a ferromagnetic beam plate with low susceptibility in an in-plane magnetic field. ASME J. Appl. Mech. 65, 121–126.

Zhou, Y.H., Zheng, X.J., 1997. A general expression of magnetic force for soft ferromagnetic plates in complex magnetic fields. Int. J. Engng. Sci. 35 (15), 1405–1417.

Zhou, Y.H., Zheng, X.J., Miya, K., 1995. Magnetoelastic bending and snapping of ferromagnetic plates in oblique magnetic field. Fusion Engng. Des. 30, 325–337.